A correlation study of layer growth rate, thickness uniformity, stoichiometry, and hydrogen impurity level of ALD grown HfO2 thin films

Blaschke, D.; Munnik, F.; Grenzer, J.; Rebohle, L.; Zahn, P.; Schmidt, H.; Gemming, S.;

Originally published:

November 2019

Applied Surface Science 506(2020), 144188

DOI: https://doi.org/10.1016/j.apsusc.2019.144188

A correlation study of layer growth rate, thickness uniformity, stoichiometry, and hydrogen impurity level in HfO_2 thin films grown by ALD between 100 °C and 350 °C

D. Blaschke[a,b,c], F. Munnik[a], J. Grenzer[a], L. Rebohle[a], H. Schmidt[b], P. Zahn[a], S. Gemming[a,c]

[a] *Institute of Ion Beam Physics and Materials Research, Helmholtz-Zentrum Dresden – Rossendorf, Bautzner Landstraße 400, 01328 Dresden, Germany*
[b] *Leibniz Institute of Photonic Technology, Albert-Einstein-Straße 9, 07745 Jena, Germany*
[c] *Institute of Physics, TU Chemnitz, 09107 Chemnitz, Germany*

Abstract

Hafnium oxide was deposited from tetrakis(dimethylamino)hafnium (TDMAHf) and water by atomic layer deposition (ALD) on heated 4″ Si wafers covered with native oxide in the temperature range from 100 °C to 350 °C. Optimized self-limiting ALD reaction and smallest hydrogen impurity level have been realized for a substrate temperature of 300 °C. The stoichiometry of deposited films and hydrogen impurity level were measured by elastic recoil detection analysis. The hafnium to oxygen ratio showed the expected 1:2 value. Besides hydrogen, no other impurities could be detected. Furthermore, a strong correlation between the growth rate per cycle (GPC), film uniformity and level of hydrogen impurities was observed.
In addition, the characterization of the crystal structure showed the appearance of some crystallites in an amorphous matrix already for a growth temperature of 250 °C and a pure crystalline layer at a growth temperature of 350 °C. The increased crystallinity with increasing growth temperature was attributed to a higher seed concentration and a nearly constant crystal size.

Keywords: atomic layer deposition, tetrakis(dimethylamido)hafnium, hafnium dioxide, elastic recoil detection analysis, hydrogen impurity level, grazing incidence X-ray diffraction

1. Introduction

Hafnium dioxide (HfO_2) is an intensively studied material which can be widely used as corrosion protection of copper [1], as antibacterial coating for medicine and biology [2], as a high-k material in electrostatic capacitors for energy storage [3], in non-volatile memories due to its ferroelectric properties [4] or the build-up and rupture of conducting filaments [5]. Furthermore, HfO_2 is frequently used as a gate oxide in MOSFETs to reduce the gate leakage currents in down scaled devices [6]. Due to the broad range of applications, a lot of research was done on the ALD growth of HfO_2 films. However, there exists much less literature about the incorporation of impurities during the ALD growth, although it is a well known problem [7, 8]. An overview about detected organic impurities in ALD grown HfO_2 films from alkylamide precursors is presented in Tab. 1. Especially, quantitative measurements of the hydrogen content are very rare. The main reason for this lies in the lack of sensitive measurement methods. Hydrogen is the most difficult chemical element to be detected in solids due to its irradiation sensitivity and its low atomic number [9]. Methods such as nuclear magnetic resonance (NMR) [10], electron paramagnetic resonance (EPR) [11], and infrared absorption spectroscopy (IR) [12] can be used to determine the content of hydrogen in solids. However, the depth-profiling in a near surface region are most commonly done by elastic recoil detection analysis (ERDA) [9, 13, 14], nuclear reaction analysis (NRA) [15–17], neutron elastic recoil detection (NERD) [18], secondary ion mass spectrometry (SIMS) [16], or by sputter-induced photon spectrometry (SIPS) [19, 20]. SIPS and SIMS suffer from the difficulty of obtaining quantitative concentrations and an induced surface roughness caused by the primary ion beam [9]. ERDA benefits from the possibility to measure several elements simultaneously in contrast to NRA. In this study, ERDA was used for a systematic investigation of the hydrogen impurity level in ALD grown HfO_2 films from the tetrakis(dimethylamido)hafnium (TDMAHf) precursor with water as O_2 source for growth temperatures between 100 °C and 350 °C. It will close the gap in literature for temperatures below 200 °C i.e. for sensitive substrates.
A literature overview of reported impurity levels and growth rates per cycle (GPC) for ALD grown HfO_2 films from several alkylamide precursors and different oxidants is given in Tab. 1. As already mentioned above, only few quantitative measurements of the H impurity level exist. Further-

*Corresponding author.
Email address: daniel.blaschke@leibniz-ipht.de (D. Blaschke)

more, no clear tendency of the achievable impurity concentration on the applied precursor, as well as the used oxidizing agent is visible. This is a result of the complex chemical processes during growth, which depend on many process parameters, like temperature, pumping speed, chamber geometry, pulse and purge times etc. A minimum GPC value of about 0.9 Å can be obtained with all three precursors in the absence of thermal precursor decomposition or parasitic CVD like processes during growth. However, the very strong correlation of the GPC and the impurity concentration causes a pronounced minimum of the impurity concentration at the smallest growth rate.
This hypothesis from Tab. 1 is confirmed by our studies and extended to include the layer thickness uniformity. Hence, the explicitly given correlations between GPC, impurity level and layer thickness uniformity provide a quality criterion, which reduces the need for direct impurity measurements to optimize the growth conditions. In addition, the crystallinity of the HfO_2 layers was investigated by grazing incidence X-ray diffraction (GIXRD) and the surface morphology was characterized by atomic force microscopy (AFM).

2. Experiment

A commercial Savannah S100 ALD system (Ultratech / Cambridge NanoTech) was used to deposit HfO_2 layers on ⟨100⟩-oriented 4″ boron doped Si wafers covered with native SiO_2 without further treatment prior to growth. Tetrakis(dimethylamido)hafnium (TDMAHf from STREM Chemicals) was used as the metal precursor, deionized H_2O as the oxygen source and N_2 as the carrier and purge gas. The ALD system was connected to a scroll vacuum pump nXDS10i (EDWARDS) and operated in continuous mode, i.e. the valve to the pumping system was always open and the carrier gas was continuously flowing while pulsing the precursor and the water. During deposition of different samples, the temperature in the ALD reaction chamber was varied from 100 °C to 350 °C in steps of 50 K. Note that for deposition temperatures of 300 °C and 350 °C only the temperature of the inner heater was set to the specified temperature, whereas the temperature of the outer heater was kept at 270 °C to protect the Kalrez O-ring sealing of the reactor against melting (Fig. 1). All other process parameters were fixed: number of cycles: n = 500, TDMAHf pulse time: 0.4 s, TDMAHf purge time: 10 s, H_2O pulse time: 0.015 s, H_2O purge time: 20 s, N_2 carrier and purge gas flow: 20 sccm, H_2O temperature in stainless steel cylinder: ambient temperature, and TDMAHf temperature in stainless steel cylinder: 75 °C. Furthermore, there was no sample rotation during the growth. We aim at a process with minimal thermal budget, so subsequent annealing was excluded from consideration.
Under these conditions, the reaction of TDMAHf with water is shown by Hausmann et al. [7] and is classified as ALD reaction with hydrogen transfer [43].

The layer thickness has been studied by spectroscopic ellipsometry (SE) at an angle of incidence of 75° using a Woollam M-2000 ellipsometer (J.A. Woollam Co., Inc.) within a spectral range from 210 to 1700 nm. Data acquisition and analysis was performed with the CompleteEASE software (J.A. Woollam Co., Inc.) by using the Tauc-Lorentz dispersion model [44] for the HfO_2 film. Surface roughness was considered by a layer based on the Bruggeman effective medium approximation [45] with 50 % voids and 50 % HfO_2. The layer thickness was determined on a grid of 13 points on every 4″ wafer, see Fig 1. The layer uniformity is defined as the standard deviation of the film thickness divided by the averaged film thickness.
In addition, X-ray reflectivity (XRR) measurements were performed to confirm the SE layer thickness. The XRR analysis was executed with a Siemens D5005 diffractometer using Cu Kα radiation with parallel beam geometry at an angle of incidence of 0° to 5°. The XRR data analysis was done with the software GenX [46]. The sample model consisted of a $HfO_2/SiO_2/Si$ stack with surface and interface roughness, density, and layer thickness as fitting parameters for the HfO_2 and SiO_2 layers.
Grazing incidence X-ray diffraction (GIXRD) data were measured at an Empyrean system from PANalytical under an angle of incidence of 1.0° using Cu Kα radiation. This data was used to estimate the crystallite size by a Williamson-Hall plot and the crystallinity (fraction of the crystalline to the amorphous phase) of the HfO_2 films by the following procedure. First of all, the background was subtracted from the GIXRD data. Afterwards, the remaining data were normalized to the film thickness. Furthermore, we assumed a pure amorphous phase for a growth temperature of 100 °C and a pure crystalline phase for a growth temperature of 350 °C. The data for growth temperatures between 150 °C and 300 °C were then fitted by a linear combination of the pure amorphous and pure crystalline diffractograms using the integral intensities, in which the coefficients give the fraction of both phases, see Supplementary Information.
The stoichiometry of the HfO_2 layers and its dependence on temperature during growth were measured by ERDA using a 43 MeV Cl^{7+} ion beam under an angle of incidence of 15°. The analyzed area was about 1.5x1.5 mm^2. The recoil ions were detected with a Bragg Ionization Chamber at a scattering angle of 31°, using a full energy detection circuit for the ion energies and a fast timing circuit to obtain a Z dependent signal to separate ion species. H was detected with a separate solid state detector at a scattering angle of 41° preceded by a 18 µm thick Al foil to stop other scattered and recoiled ions. In order to test the stability of the samples under ion bombardment during the measurement, intermediate files were saved after fixed values of the dose. The intermediate data were extrapolated to zero dose to get correction factors for the elemental losses, which allow the correct concentrations to be calculated. The fitting of measured ERDA and Rutherford backscattering spectra (RBS, Cl ions) was done simulta-

Table 1: Literature overview of reported impurity levels and GPC for ALD grown HfO_2 films from alkylamide precursors for different growth temperature ranges in comparison to this study (TS). Me = CH_3, Et = C_2H_5, DL = Detection limit, - = not measured, qualitative = measured but only relative units, XPS = X-ray photoelectron spectroscopy, FTIR = Fourier transform infrared spectroscopy, RBS = Rutherford backscattering spectrometry, AES = Auger electron spectroscopy.

				Impurities (at.%)				
Precursor	Oxidant	Temp. (°C)	GPC (Å)	C	N	H	Method	Ref.
$Hf(NMe_2)_4$	H_2O	100 – 350	1.41 – 0.88	< 0.3	< 0.1	6.2 – 1.1	ERDA	TS
$Hf(NMe_2)_4$	H_2O	205 – 400	0.89 – 2.0	2 – 3	0.6 – 1.8	5 – 7	ERDA	[21]
$Hf(NMe_2)_4$	H_2O	275	1.0	3.0	$<$ DL	qualitative	XPS, FTIR	[22]
$Hf(NMe_2)_4$	O_2 H_2O	280, 400	~ 5, ~ 14 ~ 3.5, ~ 14	qualitative	qualitative	qualitative	SIMS	[23]
$Hf(NMe_2)_4$	O_3	100, 250	1.42, 0.95	qualitative	qualitative	-	XPS	[24]
$Hf(NMe_2)_4$	O_3	250	-	$\sim 3 – 5$	qualitative	-	XPS, SIMS	[25]
$Hf(NMe_2)_4$	O_3 H_2O	300	-	qualitative $> O_3$	qualitative $> O_3$	-	SIMS	[26]
$Hf(NMe_2)_4$	H_2O	≤ 350	0.93[1]	≤ 1	≤ 0.25	-	RBS	[7]
$Hf(NMe_2)_4$	O_2 O_2-plasma H_2O	200	0.12 – 0.17[2] 1.00 – 1.10[2] 1.10	$<$ DL	$<$ DL	-	XPS	[27]
$Hf(NMeEt)_4$	O_3	275	-	1.2	< 0.4	1.5	ERDA	[28]
$Hf(NMeEt)_4$	H_2O	150 – 325	0.9 – 1.5	0.3 – 1.5	0.1 – 0.8	2 – 5	ERDA	[8]
$Hf(NMeEt)_4$	O_3 H_2O	200 – 320	1.0 – 0.8 0.85 – 0.70	10.00 – 0.74 0.76 – 0.22	- -	5.38 – 0.23 1.09 – 0.44	SIMS[3]	[29]
$Hf(NMeEt)_4$	O_3	180	1.7	~ 2.2[4]	~ 1.1[4]	~ 2.2[4]	XPS, SIMS	[30]
$Hf(NMeEt)_4$	O_3 H_2O	100	0.49 1.24	qualitative $< O_3$[5]	qualitative $< O_3$	qualitative $> O_3$	FTIR, RBS	[31]
$Hf(NMeEt)_4$	H_2O	250	1.2	2.9	$<$ DL	qualitative	XPS, FTIR	[22]
$Hf(NMeEt)_4$	O_3	200 – 275	-	1.3 – 0.08[4]	0.9 – 0.04[4]	$\sim 5.4 – 0.12$[4]	SIMS	[32]
$Hf(NMeEt)_4$	O_3	275	-	0.05 – 0.14[4]	0.04 – 0.08[4]	-	SIMS	[33]
$Hf(NMeEt)_4$	H_2O	200	0.95	~ 1	~ 1	-	XPS	[34]
$Hf(NMeEt)_4$	-	150, 300	-	~ 8.9, ~ 5.9	-	-	SIMS[6]	[35]
$Hf(NMeEt)_4$	H_2O	≤ 400	0.93[1]	≤ 1	≤ 0.25	-	RBS	[7]
$Hf(NMeEt)_4$	O_3	30 – 250	2.1 – 1.0	$\sim 10 –$ DL	$\sim 5 –$ DL	-	AES	[36]
$Hf(NMeEt)_4$	H_2O_2 H_2O	175 – 325	0.9 – 1.2 $> H_2O_2$	2 – 3 $< H_2O_2$	$<$ DL	-	AES	[37]
$Hf(NMeEt)_4$	O_3 H_2O	200, 280	1.05, 0.95 0.75	~ 10, < 5 ~ 5	$<$ DL	-	AES	[38]
$Hf(NMeEt)_4$	O_3 H_2O	150 – 300	0.94 – 0.84 1.03 – 1.12	5.15 – 0.69 7.52 – 6.22	8.23 – 7.50 0.95 – 0	-	XPS	[39]
$Hf(NMeEt)_4$	-	320 – 450	-	$\sim 6 – 2$	-	-	SIMS[6]	[5]
$Hf(NMeEt)_4$	O_3 H_2O	285 – 365	0.9 – 1.0 0.8 – 0.9	qualitative	-	-	SIMS	[40]
$Hf(NEt_2)_4$	O_2 H_2O	280, 400	~ 6.5, ~ 3.5 ~ 5, ~ 5.5	qualitative	qualitative	qualitative	SIMS	[23]
$Hf(NEt_2)_4$	H_2O	≤ 450	0.93[1]	≤ 1	≤ 0.25	-	RBS	[7]
$Hf(NEt_2)_4$	O_2-plasma O_2	250	1.3 1.0	< 2.5 ~ 5	-	-	AES	[41]
$Hf(NEt_2)_4$	H_2O	125 – 225	≥ 1.2	6 – 0	-	-	XPS	[42]

[1] purge times have been adjusted
[2] in dependence on O_2 duration
[3] RBS calibrated
[4] calculated from atoms/cm^3 using a mass density of 10.0 g/cm^3
[5] compares the impurity level with O_3 as oxidant
[6] XPS calibrated

neously using the program NDF [47].
AFM images were taken at an Agilent 5400 AFM/SPM system in tapping mode under open loop conditions. .

3. Results and Discussion

This work investigates the ALD growth of HfO_2 films from tetrakis(dimethylamido)hafnium (TDMAHf) and water in terms of growth rate per cycle (GPC), layer thickness uniformity, layer stoichiometry, and crystal structure in dependence on the growth temperature.

Fig. 1 shows the thickness variation of deposited HfO_2 films on a 4″ SiO_2/Si wafer in dependence on the growth temperature and an image of the ALD reaction chamber with the O-ring sealing, the gas inlet and outlet, and the cavity for the 4″ wafer. The thickness variation in the maps is defined as the difference between the thickness of the given measurement point and the averaged film thickness divided by the averaged film thickness. At deposition temperatures of 100 °C, 150 °C, and 200 °C the thickness variation reflects the ALD chamber symmetry with the smallest thickness between the gas inlet and outlet and an increased thickness to the sides, where the purging process is less effective due to a lower speed/rate of the N_2 purging gas. An insufficient purging results in an incomplete removal of physisorbed precursor and reaction products. Additionally, at substrate temperatures of 100 °C and 150 °C a larger thickness near the gas inlet and outlet compared to the middle of the wafer is observed. This is probably due to turbulences, which decrease the purging efficiency. An increase in deposition temperature to 250 °C leads to the most uniform HfO_2 layers of this study with a small thickness gradient perpendicular to the chamber geometry, see Fig. 2(c). The reason for this finding is not yet clear, but probably driven by some unexpected, symmetry broken gas flow during deposition due to turbulences at the gas inlet/outlet or due to a temperature gradient of the Si wafer caused by the thermal contact between wafer and ALD deposition chamber. Note that the best symmetry between gas inlet and outlet was observed for a deposition temperature of 150 °C, which is the temperature of the gas carrying pipeline. A further increase of the deposition temperature to 300 °C results in a similar thickness gradient perpendicular to the chamber geometry with a larger magnitude. The larger thickness variation than at low temperatures might be caused by a temperature gradient in the deposition chamber due to restrictions of the chamber sealing system, which allows a maximum outer heater temperature of 270 °C. Therefore, during deposition, only the temperature of the inner heater was set to 300 °C. The further increase of the thickness variation obtained at a deposition temperature of 350 °C is again driven by the increased temperature gradient between the inner and outer heater. Furthermore, the HfO_2 layer shows the largest thickness near the center of the reaction chamber, which represents the hottest area. The

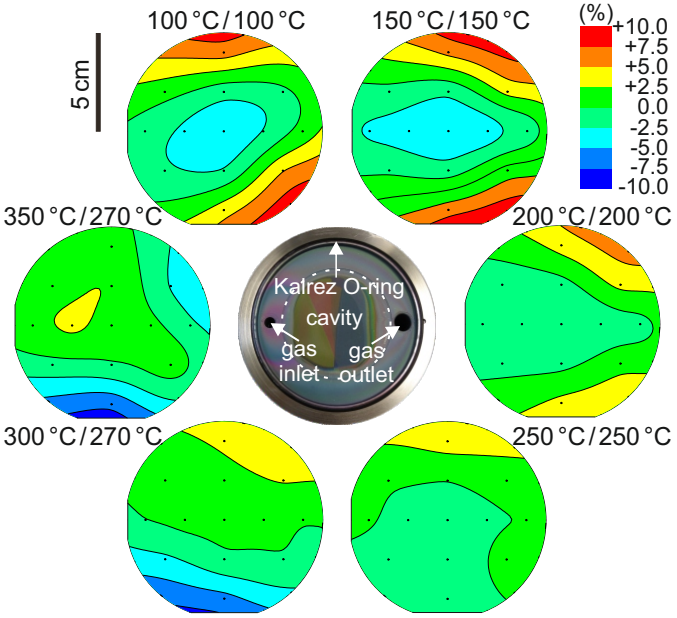

Figure 1: Maps of thickness variation between -10 % and +10 % of ALD grown HfO_2 thin films on 4″ Si wafers. The substrate temperature of the inner/outer heater has been varied between 100 °C and 350 °C in steps of 50 K. The 13 black dots in every map represent the positions of the SE measurements for the thickness determination. The film thickness variation was visualized with a Polar Contour diagram using the software OriginPro 2017 [49]. The image in the middle sketches the ALD reaction chamber with Kalrez O-ring, gas inlet, and gas outlet. The dashed white line indicates the 0.5 mm deep cavity, where the 4″ Si wafer is placed. The primary flat was parallel oriented to the virtual connection line between gas inlet and outlet during the deposition.

increased thickness is attributed to the unwanted thermal decomposition of the TDMAHf precursor [8, 29, 48].
Note that the discussion of the thickness profile depends on the reactor geometry and the dependence on the process parameters, except temperature, are not universal for other reactor types.

Fig. 2(a) shows the GPC in dependence on the deposition temperature. The values are taken from the center of the 4″ wafer. By using 500 ALD cycles, the total thickness of the HfO_2 films measured by SE is 70.7 nm, 62.0 nm, 53.8 nm, 46.7 nm, 44.2 nm, and 46.1 nm for growth temperatures between 100 °C and 350 °C, respectively. At low temperatures, the "overlapping pulses" phenomenon, which describes the simultaneous presence of the precursor and the oxidant in the gas phase near the substrate causes a non-self-limiting CVD-like growth with an increased GPC [50]. This is a result of ineffective purging, because at lower temperature a low desorption rate of physisorbed excess precursor, water and reaction by-products from the substrate or the reactor walls is obtained. With increasing growth temperatures, also the purging efficiency increases along with larger desorption rates, leading to a smaller contribution of CVD processes in the self-limiting ALD reaction and a decreased GPC. However, in addi-

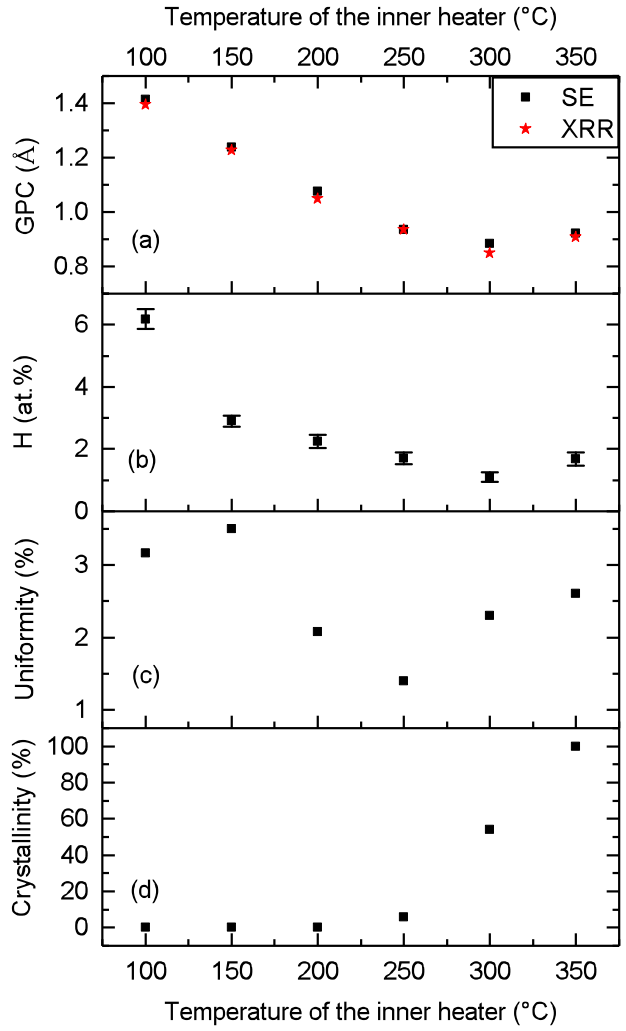

Figure 2: (a) GPC for HfO_2 thin films in dependence on deposition temperature, measured with SE (black squares) or XRR (red stars) in the middle of the wafer. (b) The H concentration in HfO_2 layers shows a similar dependence on the temperature of the inner heater as the GPC. (c) Layer thickness uniformity of the HfO_2 films on the 4″ wafer. The thickness uncertainty from the SE measurements is of the order of 0.05 nm. Therefore the error bars are of the same order as the symbol size. (d) Crystallinity of the HfO_2 films, definition see Sec. 2.

tion to the purging efficiency in ALD oxide processes, the GPC in dependence on the growth temperature can be also explained by the fact that the number of OH- groups decrease with increasing temperature and therefore also the CPC decreases [8]. The smallest GPC was observed for a growth temperature of 300 °C with a value of 0.88 Å/cycle and 0.85 Å/cycle, measured by SE and XRR, respectively. The increased GPC for a deposition temperature of 350 °C is attributed to the unwanted thermal decomposition of the hafnium precursor already in the gas phase or on the film surface, see above. Furthermore, the calculated GPC from XRR measurements was typically a bit smaller than that determined by SE. This behavior was also observed by Hausmann et al. [7]. Since the refractive index (n) and the film thickness are strongly correlated in models applied for SE analysis, uncertainties remain when one of the values is not well known [51]. XRR offers the advantage in contrast to SE that the simulation of experimental data does almost not depend on the index of refraction and the extinction coefficient (k). Hence the layer thickness determined by XRR can be used to improve further the values for n and k obtained by SE [52].

Since HfO_2 layers were deposited using a metalorganic precursor (TDMAHf), it is of interest to study the incorporation of organic species (H, C, N) into the films at different deposition temperatures. The amount of impurities and the Hf to O ratio were investigated by ERDA measurements, see Supplementary Information. The precision of the measurement is of the order of 1 at.% for Hf and O. Within the scope of this accuracy, the Hf to O ratio was determined to 1:2, independent on the growth temperature. It was not possible to detect C or N in the HfO_2 films with a concentration above the detection limit. This limit was estimated to about 0.3 at.% for C and 0.1 at.% for N and is based on a fit of the 2D background spectrum of the ERDA data (not shown). Fig. 2(b) represents the H concentration in the HfO_2 films, which follows the same trend as the GPC, shown in Fig. 2(a). This correlation between the GPC and the level of H impurities is a result of the growth mechanism. That means that a large GPC due to a non-self-limiting CVD component or thermal decomposition of the precursor during the ALD growth results in the incorporation of a high impurity level of H. The optimal ALD window which we find here, correlates with the minimum values of the GPC. Hence we propose measuring the GPC as a non-destructive fingerprint for the H impurity content of the film.

In contrast to the work of Kukli et al. [21], we observed a much smaller hydrogen content in the HfO_2 films. In the temperature range from 200 °C to 350 °C, where both works investigate the HfO_2 growth, our value of 1.1 - 2.2 at.% is in contrast to 5 - 7 at.% of Ref. [21]. Also the content of N and C was smaller in our work. This is probably due to the longer purge time after the precursor and water pulse (10/20 s vs. 0.5 s), which results in an enhanced separation of the precursor and water in the gas phase and a better removal of the excess reactants and the gaseous reaction by-products.

The layer uniformity defined in Sec. 2 is shown in Fig. 2(c). Overall, the uniformity follows a similar trend as the GPC shown in Fig. 2(a). However, for deposition temperatures of 100 °C and 300 °C there exists a discrepancy between both parameters. At 100 °C this difference probably follows from the fixed TDMAHf precursor dose, which results in an upper limit for the growth rate. Therefore, the layer thickness difference between spots on the wafer with a more efficient purging due to a higher gas flow speed/rate (between gas inlet and outlet) and spots at the wafer sides with less efficient purging conditions is limited, resulting in a better film uniformity compared to the film grown at 150 °C. At a growth temperature of 300 °C, the GPC is

still decreasing due to a more efficient purging compared to a deposition temperature of 250 °C. In contrast, the layer uniformity starts to degrade. This reflects that for growth temperatures of larger than 270 °C, the temperature of the outer heater was set to only 270 °C. Hence the temperature gradient in the ALD reaction chamber leads to a decreased film uniformity at growth temperatures of 300 °C and above. At 350 °C the decrease in layer uniformity is driven further by the thermal decomposition of the TDMAHf precursor.

Fig. 2(d) shows the crystallinity of the HfO_2 layers, which was defined above in Sec. 2. For growth temperatures up to 200 °C the layers show a pure amorphous phase. By increasing the growth temperature to 250 °C a small crystalline content of about 6 % was observed. The layer crystallinity increases to about 54 % for a growth temperature of 300 °C and shows a pure crystalline phase for a growth temperature of 350 °C.

Fig. 3 shows GIXRD patterns of the HfO_2 films in dependence on the growth temperature. For growth temperatures of 100 °C, 150 °C, and 200 °C the GIXRD data represent a pure amorphous phase. The observed sharp reflex at a 2 theta angle of about 53° corresponds to the silicon substrate. Also the reflex at about 54°, which is much weaker and appears only in some diffractograms belongs to the silicon substrate (marked with a grey background in Fig. 3). For a growth temperature of 250 °C some weak crystalline reflexes of a HfO_2 phase appear within the amorphous HfO_2 phase. These crystalline reflexes get much stronger for a growth temperature of 300 °C and even increase in intensity for a growth temperature of 350 °C, so that the amorphous phase disappears. Beside the reflex at a 2 theta angle of 30.3° (marked with an arrow), all crystalline reflexes correspond to the monoclinic HfO_2 phase. The reflex at 30.3° can be related to the cubic or orthorhombic II phase. It was estimated that this phase has a weight fraction of less than two percent. Furthermore, the crystal size was estimated by Williamson-Hall plots (Supplementary Information) to be (12.5 ± 7.1) nm and (13.1 ± 4.0) nm for a growth temperature of 300 °C and 350 °C, respectively. Due to the lack of visible crystalline reflexes for the sample grown at 250 °C, it was not possible to estimate the crystal size by this method. However, the reflex at a 2 theta angle of 28.6° has a similar FWHM as the corresponding reflex for the samples grown at higher temperatures. Hence almost no dependence of the crystal size from the growth temperature is observed.

Fig. 4 represents the surface morphology of the HfO_2 films in dependence on the growth temperature. For a growth temperature of 100 °C the surface is quite smooth with a small rms roughness of 0.38 nm. By increasing the growth temperature to 150 °C and 200 °C, most parts of the surface look like the film grown at 100 °C. However, there appear some additional spots, which are up to 12 nm higher than the rest of the film. Therefore, also the rms

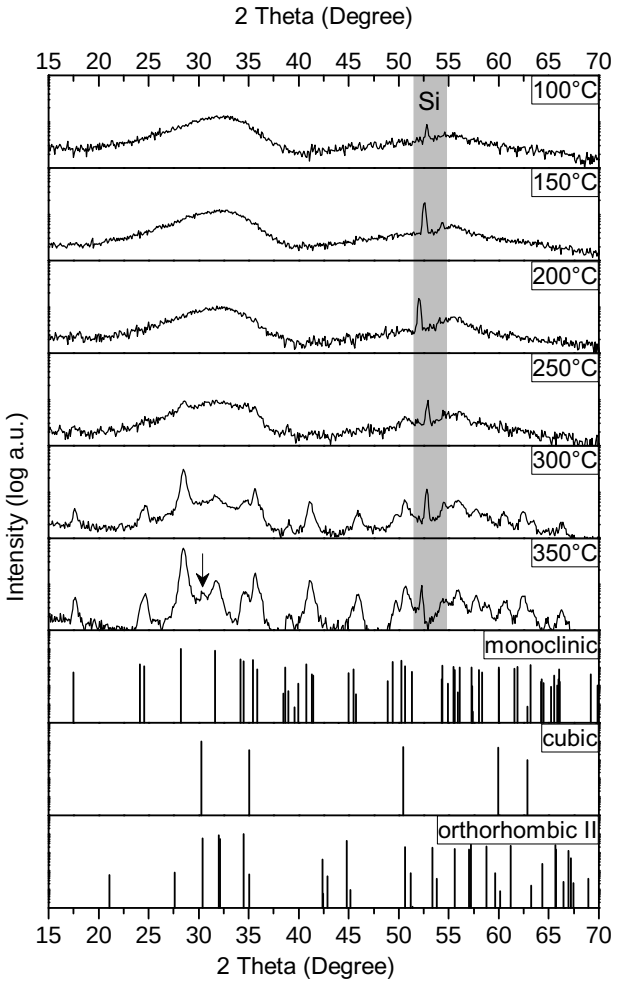

Figure 3: GIXRD patterns of HfO_2 films on Si with native oxide. The grazing incidence angle is fixed at 1.0°. The reference diffractograms are taken from Ref. [53–55] for the monoclinic, cubic and orthorhombic II phase, respectively. Si peaks from the substrate are marked with a grey background. The arrow in the GIXRD data of the HfO_2 layer grown at 350 °C shows the reflex, which is not related to the monoclinic phase.

roughness gets larger. At 250 °C the surface becomes more rough with a larger contribution from spot regions. This is deduced from the AFM height histograms provided in the Supplementary Information. The contribution of these spots increases for a temperature of 300 °C until the whole surface is covered at a temperature of 350 °C. The coalescence of the spots at 350 °C causes a decrease of the rms roughness in comparison with films grown at 250 °C and 300 °C.

The dependence of the surface roughness on the growth temperature observed during AFM measurements was confirmed by XRR and SE measurements, revealing a threshold temperature between 200 °C and 250 °C for a strong roughness increase of the HfO_2 surface. At this threshold temperature also the onset of crystallisation was observed by GIXRD measurements. Therefore, the spots in the AFM scans might be crystallites.

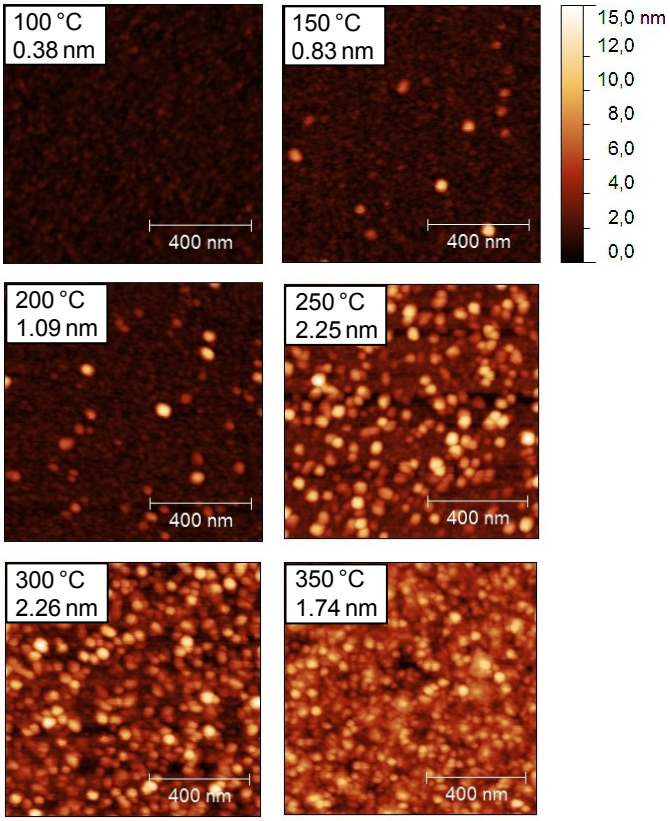

Figure 4: AFM images of the surface morphology of HfO_2 films in dependence on the growth temperature. The values in the insets represent the growth temperature and the rms roughness.

4. Conclusions

In conclusion, HfO_2 layers were successfully grown by ALD from TDMAHf and water at temperatures ranging from 100 °C to 350 °C. The hafnium to oxygen ratio was determined by ERDA as 1:2, and does not change with the growth temperature. Besides H, no other impurities such as C or N from the TDMAHf precursor could be detected. The H impurity level in the HfO_2 films shows a strong correlation with the GPC, indicating a CVD-like parasitic process or the thermal precursor decomposition during the ALD growth at larger growth rates. In addition, a correlation between the GPC and the film uniformity was observed. Based on these results we can conclude that the GPC or the film uniformity can be used as a good indicator for a chemically self-limited ALD reaction with the smallest possible amount of impurities. Within the chosen parameter set, best results can be expected at deposition temperatures between 250 °C and 300 °C.
Furthermore, GIXRD studies revealed the onset of crystallization already at a growth temperature of 250 °C and a complete crystalline layer with a dominating monoclinic phase at a growth temperature of 350 °C. The increased crystallinity with increasing growth temperature was attributed to a higher seed concentration and a nearly constant crystal size.

Acknowledgements

The authors thank Mrs. A. Scholz for the XRR measurements. Furthermore, financial support by the Initiative and Networking Fund of the Helmholtz Association (Virtual Institute MEMRIOX VH-VI-422) as well as the support by the Ion Beam Center (IBC) at HZDR is gratefully acknowledged.

References

[1] J. S. Daubert, G. T. Hill, H. N. Gotsch, A. P. Gremaud, J. S. Ovental, P. S. Williams, C. J. Oldham, G. N. Parsons, Corrosion Protection of Copper Using Al_2O_3, TiO_2, ZnO, HfO_2, and ZrO_2 Atomic Layer Deposition, ACS Appl. Mater. Interfaces 9 (4) (2017) 4192–4201. doi:10.1021/acsami.6b13571.

[2] M. Godlewski, S. Gieraltowska, L. Wachnicki, R. Pietuszka, B. S. Witkowski, A. Słońska, Z. Gajewski, M. M. Godlewski, High-k oxides by atomic layer deposition – Applications in biology and medicine, J. Vac. Sci. Technol., A 35 (2) (2017) 021508. doi:10.1116/1.4974314.

[3] L. Zhang, M. Liu, W. Ren, Z. Zhou, G. Dong, Y. Zhang, B. Peng, X. Hao, C. Wang, Z.-D. Jiang, W. Jing, Z.-G. Ye, ALD preparation of high-k HfO_2 thin films with enhanced energy density and efficient electrostatic energy storage, RSC Adv. 7 (2017) 8388–8393. doi:10.1039/C6RA27847G.

[4] A. Pal, V. K. Narasimhan, S. Weeks, K. Littau, D. Pramanik, T. Chiang, Enhancing ferroelectricity in dopant-free hafnium oxide, Appl. Phys. Lett. 110 (2) (2017) 022903. doi:10.1063/1.4973928.

[5] G. Niu, X. Cartoixà, A. Grossi, C. Zambelli, P. Olivo, E. Perez, M. A. Schubert, P. Zaumseil, I. Costina, T. Schroeder, C. Wenger, Mechanism of the Key Impact of Residual Carbon Content on the Reliability of Integrated Resistive Random Access Memory Arrays, J. Phys. Chem. C 121 (12) (2017) 7005–7014. doi:10.1021/acs.jpcc.6b12771.

[6] K. Choi, T. Ando, E. Cartier, A. Kerber, V. Paruchuri, J. Iacoponi, V. Narayanan, The past, present and future of high-k/metal gates, ECS Transactions 53 (3) (2013) 17–26. doi:10.1149/05303.0017ecst.

[7] D. M. Hausmann, E. Kim, J. Becker, R. G. Gordon, Atomic Layer Deposition of Hafnium and Zirconium Oxides Using Metal Amide Precursors, Chem. Mater. 14 (10) (2002) 4350–4358. doi:10.1021/cm020357x.

[8] K. Kukli, M. Ritala, T. Sajavaara, J. Keinonen, M. Leskelä, Atomic Layer Deposition of Hafnium Dioxide Films from Hafnium Tetrakis(ethylmethylamide) and Water, Chem. Vap. Deposition 8 (5) (2002) 199–204. doi:10.1002/1521-3862(20020903)8:5<199::AID-CVDE199>3.0.CO;2-U.

[9] J. Tirira, Y. Serruys, P. Trocellier, Forward Recoil Spectrometry: Applications to Hydrogen Determination in Solids, Plenum Press, 1996.
URL https://books.google.de/books?id=oKCyAAAAIAAJ

[10] S. Kaplan, F. Jansen, M. Machonkin, Characterization of amorphous carbonhydrogen films by solidstate nuclear magnetic resonance, Appl. Phys. Lett. 47 (7) (1985) 750–753. doi:10.1063/1.96027.

[11] D. M. Hofmann, A. Hofstaetter, F. Leiter, H. Zhou, F. Henecker, B. K. Meyer, S. B. Orlinskii, J. Schmidt, P. G. Baranov, Hydrogen: A Relevant Shallow Donor in Zinc Oxide, Phys. Rev. Lett. 88 (2002) 045504. doi:10.1103/PhysRevLett.88.045504.

[12] U. Kroll, J. Meier, A. Shah, S. Mikhailov, J. Weber, Hydrogen in amorphous and microcrystalline silicon films prepared by hydrogen dilution, J. Appl. Phys. 80 (9) (1996) 4971–4975. doi:10.1063/1.363541.

[13] J. L´Ecuyer, C. Brassard, C. Cardinal, J. Chabbal, L. Deschênes, J. P. Labrie, B. Terreault, J. G. Martel, R. St.-Jacques, An accurate and sensitive method for the determination of the depth distribution of light elements in heavy materials, J. Appl. Phys. 47 (1) (1976) 381–382. doi:10.1063/1.322288.

[14] B. L. Doyle, P. S. Peercy, Technique for profiling ^{1}H with 2.5 MeV Van de Graaff accelerators, Appl. Phys. Lett. 34 (11) (1979) 811–813. doi:10.1063/1.90654.

[15] W. A. Lanford, H. P. Trautvetter, J. F. Ziegler, J. Keller, New precision technique for measuring the concentration versus depth of hydrogen in solids, Appl. Phys. Lett. 28 (9) (1976) 566–568. doi:10.1063/1.88826.

[16] T. Lundquist, R. Burgner, P. Swann, I. Tsong, Quantitative hydrogen depth-profiling using SIMS, Appl. Surf. Sci. 7 (1) (1981) 2–6. doi:10.1016/0378-5963(81)90055-6.

[17] P. Trocellier, C. Engelmann, Hydrogen depth profile measurement using resonant nuclear reaction: An overview, J. Radioanal. Nucl. Chem. 100 (1) (1986) 117–127. doi:10.1007/BF02036505.

[18] B. Skorodumov, I. Yatsevich, Investigation of the D-Pd system interphase boundary behaviour inside the palladium by ERD using monochromatic neutrons, Nucl. Instrum. Methods Phys. Res., Sect. B 64 (1) (1992) 388–394. doi:10.1016/0168-583X(92)95501-H.

[19] I. S. T. Tsong, Photon emission from sputtered particles during ion bombardment, Phys. Status Solidi A 7 (2) (1971) 451–458. doi:10.1002/pssa.2210070219.

[20] C. Houser, J. Herman, I. Tsong, W. White, W. Lanford, Sodium-hydrogen interdiffusion in sodium silicate glasses, J. Non-Cryst. Solids 41 (1) (1980) 89–98. doi:10.1016/0022-3093(80)90194-5.

[21] K. Kukli, T. Pilvi, M. Ritala, T. Sajavaara, J. Lu, M. Leskelä, Atomic layer deposition of hafnium dioxide thin films from hafnium tetrakis(dimethylamide) and water, Thin Solid Films 491 (1) (2005) 328–338. doi:10.1016/j.tsf.2005.05.050.

[22] J. C. Hackley, T. Gougousi, Properties of atomic layer deposited HfO_2 thin films, Thin Solid Films 517 (24) (2009) 6576–6583. doi:10.1016/j.tsf.2009.04.033.

[23] S. Hino, M. Nakayama, K. Takahashi, H. Funakubo, E. Tokumitsu, Characterization of Hafnium Oxide Thin Films by Source Gas Pulse Introduced Metalorganic Chemical Vapor Deposition Using Amino-Family Hf Precursors, Jpn. J. Appl. Phys. 42 (9B) (2003) 6015–6018. doi:10.1143/JJAP.42.6015.

[24] T. J. Park, Y. Byun, R. M. Wallace, J. Kim, Reduced impurities and improved electrical properties of atomic-layer-deposited HfO_2 film grown at a low temperature (100 °C) by Al_2O_3 incorporation, Appl. Surf. Sci. 371 (2016) 360–364. doi:10.1016/j.apsusc.2016.02.243.

[25] T. J. Park, K. J. Chung, H.-C. Kim, J. Ahn, R. M. Wallace, J. Kim, Reduced Metal Contamination in Atomic-Layer-Deposited HfO_2 Films Grown on Si Using O_3 Oxidant Generated Without N_2 Assistance, Electrochem. Solid-State Lett. 13 (8) (2010) G65–G67. doi:10.1149/1.3430657.

[26] M. Cho, D. S. Jeong, J. Park, H. B. Park, S. W. Lee, T. J. Park, C. S. Hwang, G. H. Jang, J. Jeong, Comparison between atomic-layer-deposited HfO_2 films using O_3 or H_2O oxidant and $Hf[N(CH_3)_2]_4$ precursor, Appl. Phys. Lett. 85 (24) (2004) 5953–5955. doi:10.1063/1.1829773.

[27] J. Provine, P. Schindler, J. Torgersen, H. J. Kim, H.-P. Karnthaler, F. B. Prinz, Atomic layer deposition by reaction of molecular oxygen with tetrakisdimethylamido-metal precursors, J. Vac. Sci. Technol., A 34 (1) (2016) 01A138. doi:10.1116/1.4937991.

[28] J. Niinistö, M. Mäntymäki, K. Kukli, L. Costelle, E. Puukilainen, M. Ritala, M. Leskelä, Growth and phase stabilization of HfO_2 thin films by ALD using novel precursors, J. Cryst. Growth 312 (2) (2010) 245–249. doi:10.1016/j.jcrysgro.2009.10.028.

[29] X. Liu, S. Ramanathan, A. Longdergan, A. Srivastava, E. Lee, T. E. Seidel, J. T. Barton, D. Pang, R. G. Gordon, ALD of Hafnium Oxide Thin Films from Tetrakis(ethylmethylamino)hafnium and Ozone, J. Electrochem. Soc. 152 (3) (2005) G213–G219. doi:10.1149/1.1859631.

[30] Y. Kim, Y. Roh, J.-B. Yoo, H. Kim, Characteristics of atomic layer deposition grown HfO_2 films after exposure to plasma treatments, Thin Solid Films 515 (5) (2007) 2984–2989. doi:10.1016/j.tsf.2006.08.039.

[31] Y. Wang, M. Dai, M.-T. Ho, L. S. Wielunski, Y. J. Chabal, Infrared characterization of hafnium oxide grown by atomic layer deposition using ozone as the oxygen precursor, Appl. Phys. Lett. 90 (2) (2007) 022906. doi:10.1063/1.2430908.

[32] S. Kamiyama, T. Miura, Y. Nara, Electrical properties of ultrathin HfO_2 films for replacement metal gate transistors, fabricated by atomic layer deposition using $Hf(N(CH_3)(C_2H_5))_4$ and O_3, Appl. Phys. Lett. 87 (13) (2005) 132904. doi:10.1063/1.2072827.

[33] S. Kamiyama, T. Miura, Y. Nara, Impact of O_3 Concentration on Ultrathin HfO_2 Films Deposited on HF-Cleaned Silicon Using Atomic Layer Deposition with $Hf[N(CH_3)(C_2H5)]_4$, Electrochem. Solid-State Lett. 9 (9) (2006) G285–G288. doi:10.1149/1.2217134.

[34] Y.-K. Chiou, C.-H. Chang, T.-B. Wu, Characteristics of hafnium oxide grown on silicon by atomic-layer deposition using tetrakis(ethylmethylamino)hafnium and water vapor as precursors, J. Mater. Res. 22 (2007) 1899–1906. doi:10.1557/jmr.2007.0242.

[35] G. Niu, H.-D. Kim, R. Roelofs, E. Perez, M. A. Schubert, P. Zaumseil, I. Costina, C. Wenger, Material insights of HfO_2-based integrated 1-transistor-1-resistor resistive random access memory devices processed by batch atomic layer deposition, Sci. Rep. 6 (2016) 28155. doi:10.1038/srep28155.

[36] J. H. Kim, T. J. Park, S. K. Kim, D.-Y. Cho, H.-S. Jung, S. Y. Lee, C. S. Hwang, Chemical structures and electrical properties of atomic layer deposited HfO_2 thin films grown at an extremely low temperature ($\leq$ 100 °C) using O_3 as an oxygen source, Appl. Surf. Sci. 292 (2014) 852–856. doi:10.1016/j.apsusc.2013.12.061.

[37] M.-J. Choi, H.-H. Park, D. S. Jeong, J. H. Kim, J.-S. Kim, S. K. Kim, Atomic layer deposition of HfO_2 thin films using H_2O_2 as oxidant, Appl. Surf. Sci. 301 (2014) 451–455. doi:10.1016/j.apsusc.2014.02.098.

[38] S. Y. Lee, H. K. Kim, J. H. Lee, I.-H. Yu, J.-H. Lee, C. S. Hwang, Effects of O_3 and H_2O as oxygen sources on the atomic layer deposition of HfO_2 gate dielectrics at different deposition temperatures, J. Mater. Chem. C 2 (2014) 2558–2568. doi:10.1039/C3TC32561J.

[39] J. Fan, H. Liu, Q. Kuang, B. Gao, F. Ma, Y. Hao, Physical properties and electrical characteristics of H_2O-based and O_3-based HfO_2 films deposited by ALD, Microelectron. Reliab. 52 (6) (2012) 1043–1049. doi:10.1016/j.microrel.2012.01.010.

[40] J. Swerts, N. Peys, L. Nyns, A. Delabie, A. Franquet, J. W. Maes, S. Van Elshocht, S. De Gendt, Impact of Precursor Chemistry and Process Conditions on the Scalability of ALD HfO_2 Gate Dielectrics, J. Electrochem. Soc. 157 (1) (2010) G26–G31. doi:10.1149/1.3258664.

[41] S. Choi, J. Koo, H. Jeon, Y. Kim, Plasma-Enhanced Atomic-Layer Deposition of a HfO_2 Gate Dielectric, J. Korean Phys. Soc. 44 (1) (2004) 35–38.

[42] Q. Tao, G. M. Jursich, C. Takoudis, Investigation of Surface Sputtering and Post Annealing Effects on Atomic Layer Deposited HfO_2 and TiO_2, IEEE Trans. Semicond. Manuf. 24 (2) (2011) 139–144. doi:10.1109/TSM.2011.2106167.

[43] R. G. Gordon, Atomic Layer Deposition for Semiconductors, Springer Science & Business Media, New York, 2014, Ch. 2. ALD Precursors and Reaction Mechanisms, pp. 15–46. doi:10.1007/978-1-4614-8054-9.

[44] G. E. Jellison Jr., F. A. Modine, Parameterization of the optical

functions of amorphous materials in the interband region, Appl. Phys. Lett. 69 (3) (1996) 371–373. doi:10.1063/1.118064.

[45] D. A. G. Bruggeman, Berechnung verschiedener physikalischer Konstanten von heterogenen Substanzen. I. Dielektrizitätskonstanten und Leitfähigkeiten der Mischkörper aus isotropen Substanzen, Ann. Phys. 416 (7) (1935) 636–664. doi:10.1002/andp.19354160705.

[46] M. Björck, G. Andersson, GenX: an extensible X-ray reflectivity refinement program utilizing differential evolution, J. Appl. Cryst. 40 (2007) 1174–1178. doi:10.1107/S0021889807045086.

[47] N. P. Barradas, C. Jeynes, R. P. Webb, Simulated annealing analysis of Rutherford backscattering data, Appl. Phys. Lett. 71 (2) (1997) 291–293. doi:10.1063/1.119524.

[48] T. Kääriäinen, D. Cameron, M.-L. Kääriäinen, A. Sherman, Atomic Layer Deposition: Principles, Characteristics, and Nanotechnology, John Wiley & Sons, Hoboken, 2013, Ch. 1. Fundamentals of Atomic Layer Deposition, pp. 1–31. doi:10.1002/9781118747407.ch1.

[49] OriginPro 2017 (OriginLab, Northampton, MA).

[50] K.-E. Elers, T. Blomberg, M. Peussa, B. Aitchison, S. Haukka, S. Marcus, Film Uniformity in Atomic Layer Deposition, Chem. Vap. Deposition 12 (1) (2006) 13–24. doi:10.1002/cvde.200500024.

[51] S. Ferrari, M. Modreanu, G. Scarel, M. Fanciulli, X-Ray reflectivity and spectroscopic ellipsometry as metrology tools for the characterization of interfacial layers in high-κ materials, Thin Solid Films 450 (1) (2004) 124–127. doi:10.1016/j.tsf.2003.10.051.

[52] J. P. Cain, S. Robie, Q. Zhang, B. Singh, I. Emami, Combined use of X-ray reflectometry and spectroscopic ellipsometry for characterization of thin film optical properties, in: Proc. of SPIE, Vol. 6155, 2006, p. 61550P. doi:10.1117/12.660088.

[53] D. Shin, R. Arroyave, Z. K. Liu, Thermodynamic modelling of the Hf-Si-O system, Calphad 30 (2006) 375–386. doi:10.1016/j.calphad.2006.08.006.

[54] N. G. Gorashchenko, V. I. Ivanovskaya, A. A. Maier, N. I. Markov, N. R. Miftyakhetdinova, V. A. Myzina, V. V. Osiko, V. M. Tatarintsev, Properties of solid-solution single crystals in HfO_2-Ln_2O_3 systems (Ln= Y, rare earths), Inorg. Mater. 21 (1985) 1323–1326.

[55] J. Tang, M. Kai, Y. Kobayashi, S. Endo, O. Shimomura, T. Kikegawa, T. Ashida, A High-Pressure High-Temperature X Ray Study of Phase Relations and Polymorphism of HfO_2, in: Properties of Earth and Planetary Materials at High Pressure and Temperature, 1st Edition, American Geophysical Union, Washington, D. C., 1998.